

Novel Photovoltaic Systems with Power Sensor-less MPPT Approaches for AC Mains Interface

Mikihiko Matsui^{*1} and Tatsuya Kitano^{*2}

MPPT (maximum power point tracking) control is very important for the practical PV (photovoltaic) systems to maintain efficient power generating conditions irrespective of the deviation in the PV array insolation or/and temperature conditions. Although a plenty of researches have been done so far, most of them are too costly because of much dependence on expensive sensors for measuring photovoltaic power and micro-processors for achieving elaborate and complicated control strategies. From this point of view, authors have been researching on sensor-less approaches for MPPT control, and have proposed two types of new control schemes "Power Equilibrium Scheme" and "Limit Cycle Scheme". This paper summarises these two schemes with focussing on their operating principles and some results of simulation and experiments.

1. Introduction

In order to track the time varying maximum power point of the solar array depending on its operating conditions of insolation and temperature, the MPPT (maximum power point tracking) control technique plays an important role in the practical PV systems. A variety of MPPT schemes have been proposed in the literatures so far [1]-[3]. Some of them are applying fuzzy logic, neural networks, GA (genetic algorithm) techniques, etc. in order to achieve a fast response in the transient state and a stable operation in the steady state at the same time. These new approaches seem to be very useful in some special cases from a viewpoint of their control quality. However, they are too costly for most cases because they are too dependant on expensive sensors and micro-processors. Therefore, the simpler approaches have been required for the most of practical mass-produced PV systems.

Standing on this point of view, the authors have been focussing on the simplification of the MPPT control system by utilizing steady state power balancing condition at dc link which is the inter-link stage of two power conversion stages, i.e. a boost chopper stage and a PWM inverter stage. Then, two types of new power sensor-less MPPT control schemes, referred as "Type-1 Power Equilibrium

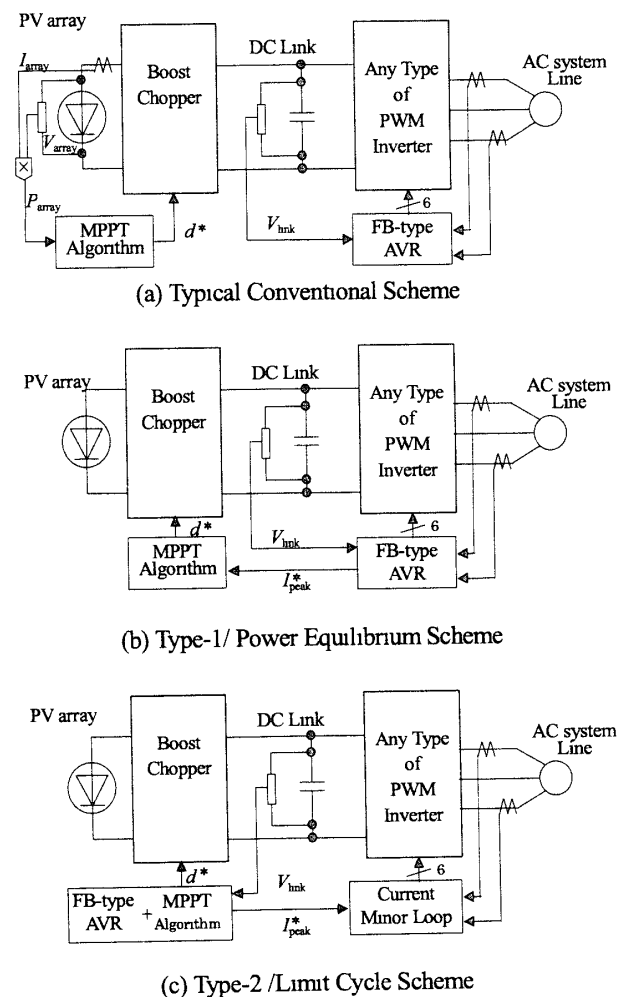


Fig 1 Conventional and two types of proposed MPPT schemes

^{*1} Associate professor Dept. of Electronics and Computer Engineering, Faculty of Engineering, Tokyo Institute of Polytechnics

^{*2} Ph.D candidate Graduate School of Electronics and Computer Engineering, Tokyo Institute of Polytechnics

Scheme" and "Type-2: Limit Cycle Scheme" in this paper, have been proposed [4]-[8]. Fig.1 shows the block diagrams of a typical conventional MPPT system and the two types of proposed systems. The proposed two systems both utilize the sensors for dc link voltage detection and ac current detection which are indispensable for the inverter system itself, and need no additional sensors for PV array power detection.

This paper summarizes the basic principles of these new sensor-less approaches proposed by the author and validates the availability of the systems by showing some simulation and experimental results.

2. Type-1/Power Equilibrium Scheme

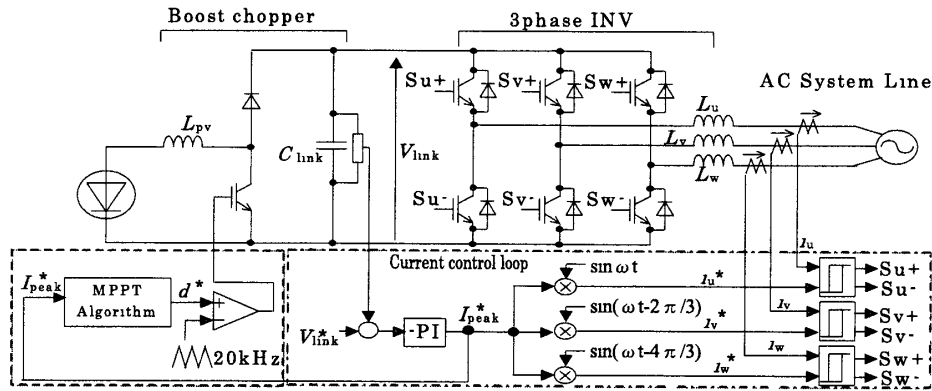


Fig 2 System configuration of Type-1, "Power Equilibrium Scheme"

2.1 Basic Operation principles

Fig 2 shows the system configuration of Type-1. For the typical conventional MPPT control schemes, it is essential to use the information of actual output power of the PV array, and the duty ratio for boost chopper is selected to maximize the output power by MPPT algorithm. On the other hand, this system need not depend on the information of actual power. In the steady state condition, the generated power of the solar array and the regenerative power flow toward the ac system should have a balance. Therefore, the generated power P_{array} is in proportion to inverter output current magnitude command I_{peak}^* which is the inner signal of the control loop in the steady state as shown in Fig 3. Therefore, MPPT

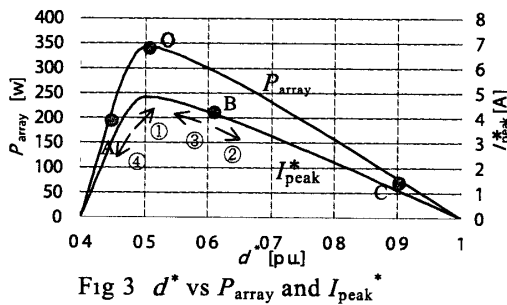


Fig 3 d^* vs P_{array} and I_{peak}^*

Table1 Operating direction of d^* in MPPT control

Operating Points in Fig 3	Current States		Operating direction of d^*
	I_{peak}^*	d^*	
①	Positive	Increasing	Hold on
②	Negative	Increasing	Turn over
③	Positive	Decreasing	Hold on
④	Negative	Decreasing	Turn over

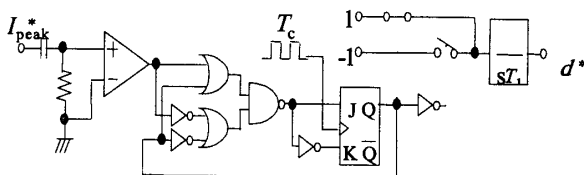


Fig 4 Example of a simple hardware implementation for Type-1 MPPT control

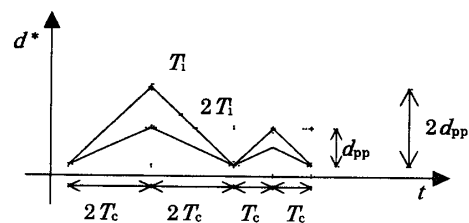


Fig 5 Relations between T_1 , T_c and d^*

operation is achieved by maximizing I_{peak}^* in place of d^*

For an easy implementation of the MPPT algorithm, a simple electronic circuit shown in Fig 4 has been examined here. Based on the differential value for the time dependent variable $d(I_{peak}^*)/dt$, the searching direction whether increasing or decreasing the value of d^* is determined every sampling time T_c . That is, if I_{peak}^* is increasing, the searching direction is always kept constant as before irrespective of the current state of d^* (Fig 3-① and Fig.3-③). On the other hand, if the differential value of I_{peak}^* is found to be negative at a sampling time, then the searching direction is changed irrespective of the current state of d^* (Fig 3-② and Fig 3-④). This decision making is arranged in the Table 1. Fig.5 shows the relationships between the integrator time constant T_i , sampling time T_c and duty ratio command d^* . T_i and T_c are the design parameters which are selected later based on Fig 9.

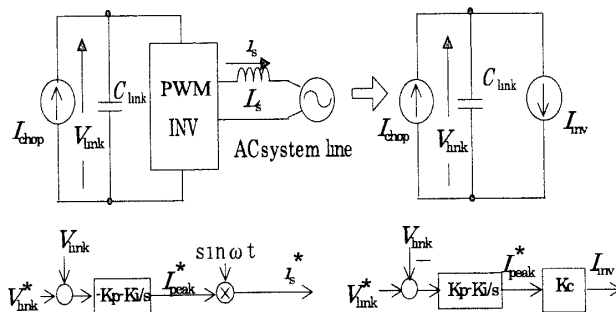


Fig 6 Modeling of inverter

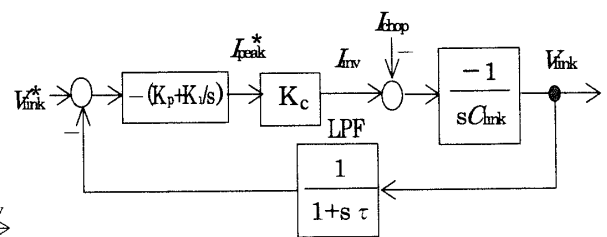


Fig 7 Dc link voltage control loop

2.2 System Designing Approaches

The parameters of the main circuit and those of the controller are determined from the practical viewpoint to ensure well-damped stable operation and the sufficient quick response. For this purpose, state space averaging model is deduced by neglecting the switching phenomena of chopper and inverter stages as shown in Fig 6. Then the block diagram representation in Fig 7 can be derived. Where, the time delay τ of a first order LPF (low-pass filter) represents the equivalent total time delay of the control loop. In the case of $\tau=0$, the system becomes a two-order system. Assuming that the two poles are assigned at a same place $-\alpha$, whereas α is a positive real value, the equivalent time-lag τ_{pi} of the PI control loop becomes $2/\alpha$. In the practical system, the time constant τ is given at first. Fig 8 shows an effect of τ on the step response waveform against disturbance. It is clear that τ_{pi} should be selected at least 5 times greater than τ . The larger PI control gains enable the faster response, but the damping become worse. For this reason, it is an important criterion to give the upper limit of the PI gains and ensure well damped operation of the system.

Once the τ_{pi} is determined, the time constant T_i and T_c are selected to suppress the peak to peak value of duty ratio d_{pp} based on the relationships shown in Fig 9. Here, two cases I and II are selected as examples.

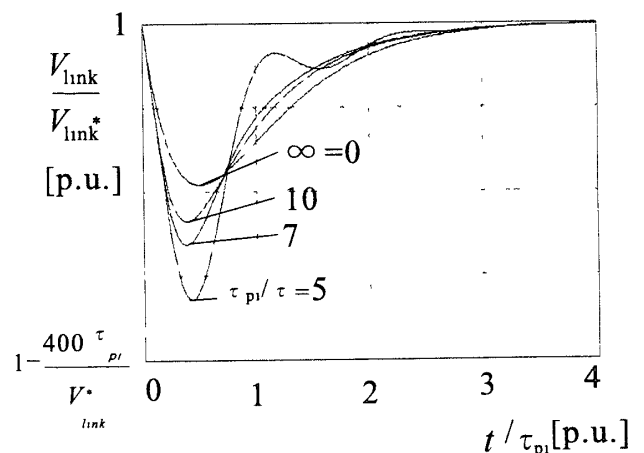


Fig 8 Step Response against disturbance

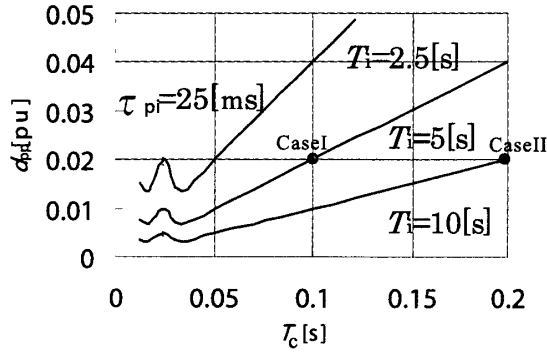
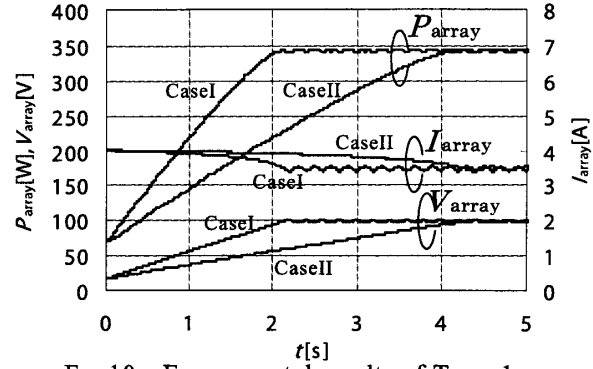
Fig 9 Relations between T_c and dpp

Fig 10 Experimental results of Type-1

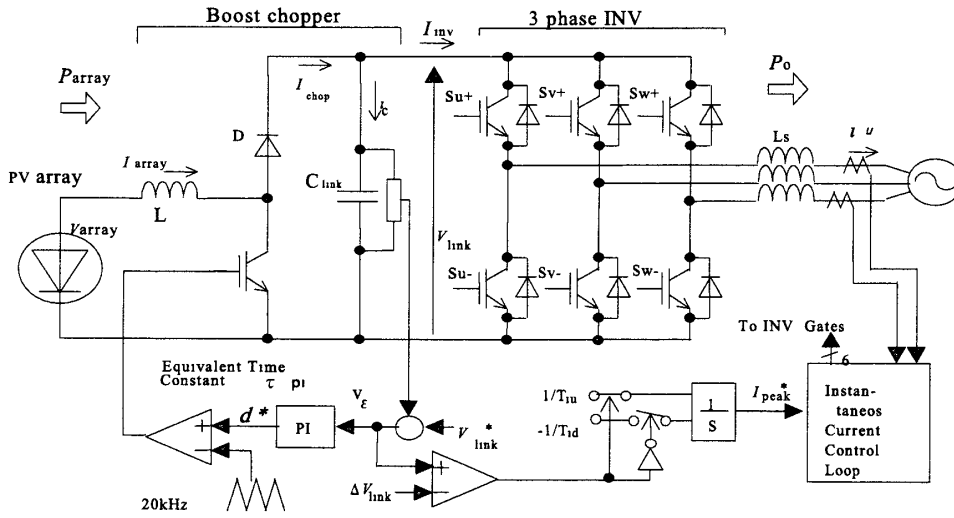


Fig 11 System configuration of Type-2

"Limit Cycle Scheme"

2.3 Experimental Results

In the experiment, a solar array simulator (Hewlett Packard E4351B) has been used to realize reproducible time varying insolation conditions of the PV array. A set of different v-p curves corresponding to the changing insolation conditions have been programmed.

Fig.10 shows examples of step responses for two cases, A and B. They successfully track the maximum power point. The response time has been proved fast enough for the practical use.

3. Type-2/Limit Cycle Scheme

3.1 Basic Operation principles

Fig.11 shows the system configuration of Type-2. This approach is characterized by its complete removal of the conventional "mountain climbing algorithm" to optimize the operating point. As a result, the control circuit becomes extremely simple, and it is suited for very low-cost small-sized systems such as ac modules, and the pumping motor systems combined with PV arrays.

The basic operation principles are explained by using Fig.11 and the operating waveforms are shown in Fig 12. In this system, the dc link voltage between two power conversion stages is kept constant by the PI control loop on the left hand chopper side. At the same time, the link voltage error signal is also observed by the comparator in the load leveling loop on right hand inverter side. The loading level against the PV array is adjusted by changing the ac current amplitude command I_{peak}^* . This system realizes such an operation only by switching the input terminal of the integrator with two different values, $+1/T_{iu}$ and

$-1/T_{id}$, based on the result of error signal comparison

Assuming the switch is connected to the positive side $+1/T_{iu}$ at first, I_{peak}^* may start to rise up gradually as shown in Fig 12. Unless the output power P_{array} reaches to the maximum power point P_{max} of the array, the dc link voltage V_{link} may be kept constant with the help of PI control loop on chopper side. However, once P_{array} has reached to P_{max} , V_{link} could no longer be kept constant because the power equilibrium cannot be maintained. Thus, V_{link} begins to go down, and the voltage error signal may soon become larger than a preset small value ΔV_{link} . Then, the switch is turned over to the negative side $-1/T_{id}$, and the I_{peak}^* begins to decrease. Then, V_{link} gradually stops decreasing and again begins to increase. In this way, a kind of non-linear oscillation, so-called "limit cycle", occurs on the equilibrium/non-equilibrium boundary of the system power flow around the maximum power operating point. The generated output power on ac system side can be automatically maximized without using any information of voltage and/or current on PV array side.

Fig 13 shows an example of a simple hardware implementation for this control scheme.

3.2 System Designing Approaches

In order to ensure the stable operation, i.e. to guarantee the occurrence of the limit cycle, it is an important design criterion to give an adequate relationship between the time constants T_{iu} , T_{id} and the equivalent time-lag of the PI control loop, τ_{pi} . That is, the relationship, $T_{id} > \tau_{pi} > T_{iu}$, should hold.

Fig 14 shows approximate wave forms of limit cycle operation based on a state space averaging model ignoring the high frequency switching phenomena. Basing on these waveforms, the relation between the system parameters and the resulted limit cycle frequency, amplitude of the limit cycle ripple component can be derived.

According to the latest detailed investigations [6], the limit cycle frequency does not depend on the insolation conditions. But the equivalent time-lag of the PI control loop, τ_{pi} changes in proportion to the

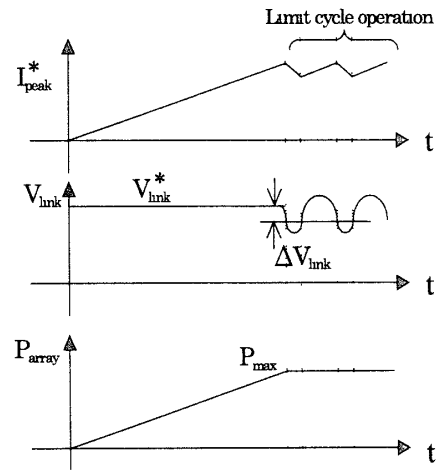


Fig 12 Principle of MPPT operation utilizing limit cycle

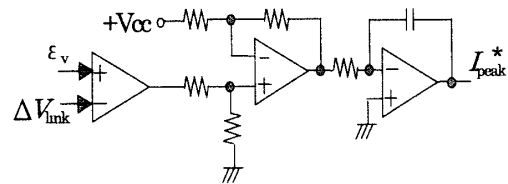


Fig 13 Example of a simple hardware implementation for Type-2 MPPT control

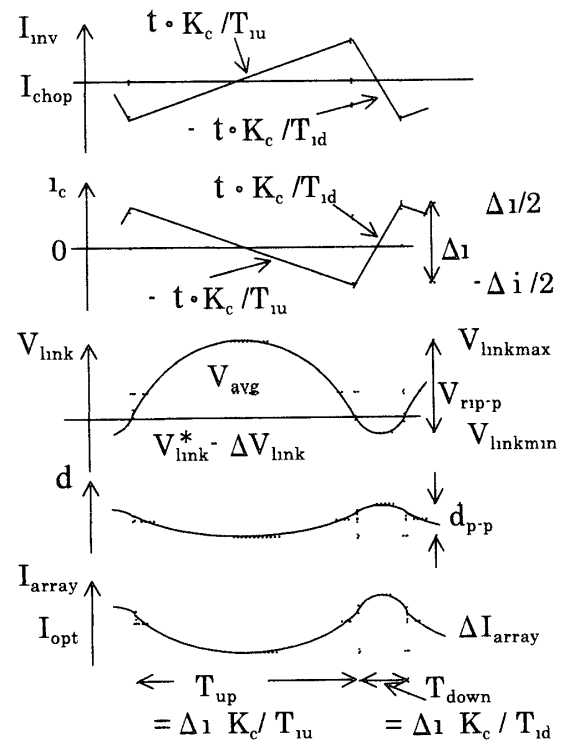


Fig 14 Approximate waveforms during limit cycle operation

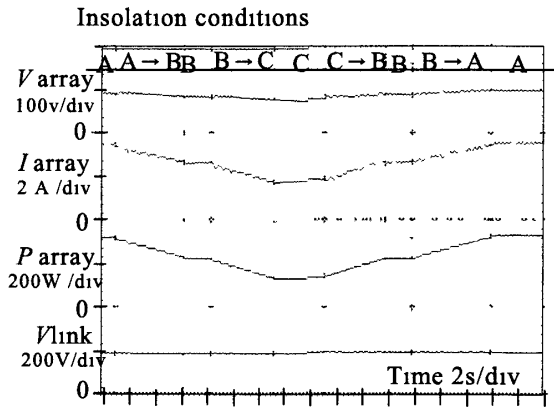


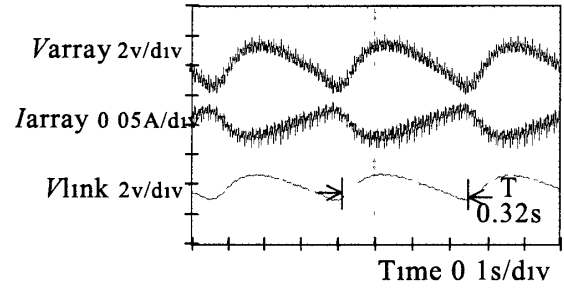
Fig 15 Experimental operating waveforms of Type-2 insolation. For this reason, T_{iu} should be selected smaller than the minimum value of t_{pi} in operation, say $0.2p.u.$ against the maximum insolation condition. For the lower insolation than $0.2p.u.$, the MPPT operation using limit cycle is no longer useful, and the operating mode can be automatically switched to "constant voltage mode" simply by giving the upper limit value for d^* with an additional limiter. In this mode of operation, V_{link} is maintained almost constant around the voltage command with the help of inverter side feedback loop. Therefore, the dc link voltage has never been corrupted or discharged over even if the photovoltaic power decreased to be complete zero.

3.3 Experimental Results

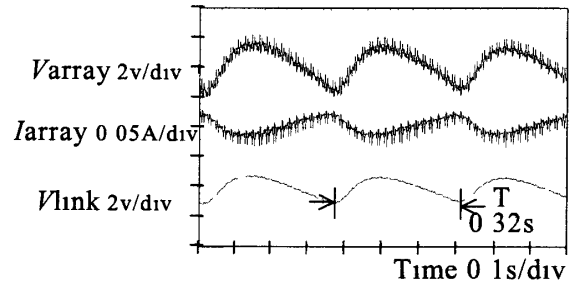
Three different patterns of v-p curves, A ($V_o=120[V]$, $I_{sc}=4[A]$), B ($V_o=110[V]$, $I_{sc}=3[A]$), C ($V_o=100[V]$, $I_{sc}=2[A]$), corresponding to the changing insolation conditions have been programmed in a solar array simulator (Hewlett Packard E4351B) to realize reproducible experiment.

Fig.15 shows an experimental response waveforms when the insolation condition has gradually changed as $A \rightarrow B \rightarrow C \rightarrow B \rightarrow A$. A successful track to the maximum power point can be observed. Fig.16 shows the expanded experimental waveforms of limit cycle operation for conditions A and C, respectively. It can be seen that the limit cycle frequency is almost same, around 3[Hz], for both conditions.

A full-daytime test has been carried out by using a photovoltaic array shown in Fig 17 with 1.5 [kW] rating



(a) Insolation condition A



(b) Insolation condition C

Fig 16 Experimental waveforms of limit cycle operation

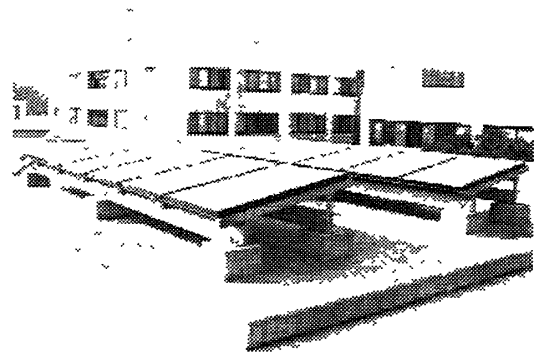


Fig 17 1.5kW photovoltaic array on the roof of the JRCH building in T.I.P

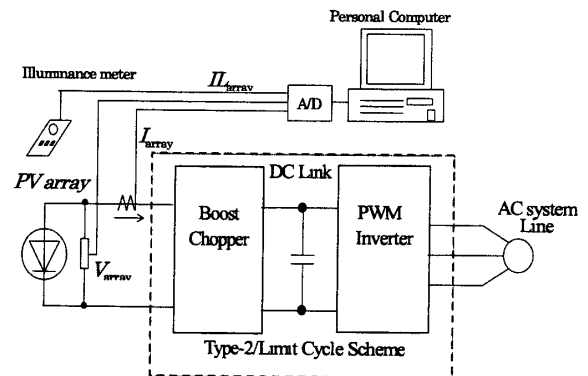


Fig. 18 Instrumentation system for full-daytime testing of Type-2 system.

which is settled on the top roof of the JRCH (Joint Research Center for High-technology) building in Tokyo Institute of Polytechnics in Atsugi-city Kanagawa, Japan. The configuration of measuring instrumentation system is shown in Fig. 18. An A/D converter board has been connected with the personal computer, and the data logging has been done every five-second. The input data to the A/D converter include the insolation measured by an illuminance meter, voltage and current of the solar array. The measurement has been carried out for nine hours from 8:00 a.m. to 17:00 p.m. on April 20, 2001. The measured data, i.e. illuminance (ILarray), solar array voltage, current, and calculated power are shown in Fig. 19. The optimal operating voltage which is slightly changing with the insolation of the PV array is successfully tracked with stable operation.

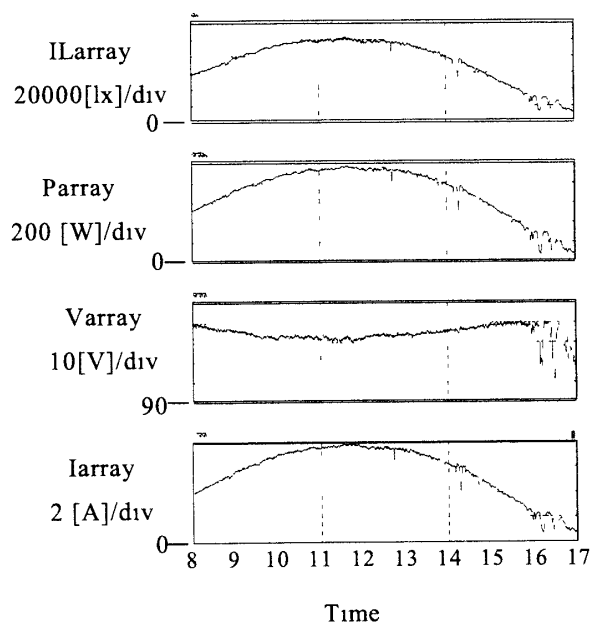


Fig. 19 Insolation, Parray, Varray and Iarray.

4. Conclusions

This paper has summarized two types of new power sensor-less MPPT control schemes previously proposed by the authors, referred as "Type-1/ Power Equilibrium Scheme" and "Type-2/ Limit Cycle Scheme" in this paper. Because of the short pages, special care has been taken to explain the basic principles of the ideas, particular problems to be solved and the stances for approaching the problems for both new schemes without using equations. The qualitative detailed investigations have been given in the references [6]-[8].

The importance of utilizing the renewable energy system, including photovoltaic system and wind turbine generation system etc., has been attracted greatly in these days. Although the total energy amount is still small, it is also important in the sense of enlightening the public people to know the benefit of energy and importance of saving it through their daily life. For this purpose, continuous effort to develop more attracting systems with lower-cost, higher-performance and multi-functions are required. Sensor-less approach explained in this paper is one of such key aspects.

Acknowledgment

This work has been supported by 2001 Grant-in-Aid for Scientific Research from the MEXT (ministry of education, culture, sports, science and technology) of Japan, and the JRCH(Joint Research Center for High-technology) of Tokyo Institute of Polytechnics. The authors would like to thank all the people who are concerned

References

- [1] B.K.Bose, P.M.Szczesny and R.L.Steigerwalt, "Microcomputer control of a residential power conditioning system," IEEE Trans Industrial Applications, Vol 21, No. 5, Oct. 1985, pp. 1182-1191.
- [2] T.Senju, K Uezato and S Okuma, "Maximum power tracking control of photovoltaic array using fuzzy control," IEEJ Trans Vol.9, No.D-114, 1994, pp.843-848.
- [3] H Sugimoto and H.A.Dong, "A new scheme for maximum photovoltaic power tracking control," in Proceedings of the 1997 PCC-Nagaoka, Vol.2, pp.691-696.
- [4] M Matsui, T.Kitano, D.H.Xu and Z Q.Yang, "A New Maximum Photovoltaic Power Tracking Control Scheme Based on Power Equilibrium at DC Link ," in Proceedings of the 1999 IEEE IAS Annual Meeting, pp 804-809.
- [5] M.Matsui, T.Kitano, D.H.Xu and Z Q.Yang, "New MPPT Control Scheme Utilizing Power Balance at DC Link Instead of Array Power Detection," in Proceedings of the 2000 IEEJapan IPEC-Tokyo, Vol 1, pp. 164-169.
- [6] T.Kitano, M.Matsui and D H.Xu, "A MPPT Control Scheme for PV System Utilizing Limit Cycle Operation - System Design to Ensure Stability and Responce -," Presented at The Symposium of Japan Society for Power Electronics, JSPE-27-12,2001· in press in Japanese
- [7] T Kitano, M Matsui and D H.Xu, "Power Sensor-less MPPT Control Scheme Utilizing Power Balance at DC Link - System Design to Ensure Stability and Response -, " in Proceedings of the 2001 IEEE IECON(Denver) , 2001
- [8] T.Kitano, M.Matsui and D H.Xu,"A Maximum Power Point Tracking Control Scheme for PV System Based on Power Equilibrium and Its System Design ," IEEJ Trans , Vol.121-D, No 12, 2001 : in press in Japanese